Organic Electronics 10 (2009) 769–774

Contents lists available at ScienceDirect

Organic Electronics

journal homepage: www.elsevier.com/locate/orgel

An optical programming/electrical erasing memory device: Organic thin film transistors incorporating core/shell CdSe@ZnSe quantum dots and poly(3-hexylthiophene)

Mao-Yuan Chiu [a], Chen-Chia Chen [a], Jeng-Tzong Sheu [b], Kung-Hwa Wei [a,*]

[a] Department of Materials Science and Engineering, National Chiao Tung University, 1001 Ta Hsueh Road, Hsinchu 30050, Taiwan, ROC
[b] Institute of Nanotechnology, National Chiao Tung University, 1001 Ta-Hsueh Road, Hsinchu 30050, Taiwan, ROC

ARTICLE INFO

Article history:
Received 27 February 2009
Received in revised form 26 March 2009
Accepted 26 March 2009
Available online 2 April 2009

PACS:
85.60.Dw
85.30.Tv
82.35.Np

Keywords:
Organic thin film transistor
Memory
Conjugated polymers
Quantum dot
Core/shell

ABSTRACT

An optical programming/electrical erasing memory device was fabricated by adopting organic thin film transistors incorporating core/shell CdSe@ZnSe quantum dots (QDs) and poly(3-hexylthiophene) (P3HT) as active layers. After illumination, the presence of quantum well-structured core/shell CdSe@ZnSe QDs within the P3HT film enhanced the maximum ON/OFF ratio substantially to 2700; this value was maintained for 8000 s without noticeable decay. The ON state current could be erased effectively when using a single pulse of the gate voltage (−10 V). This fabrication approach opens up the possibility of improving the memory performance of polymeric materials prepared at low cost using simple processes.

1. Introduction

The development of conjugated polymers for use in organic optoelectronic devices is an area of intense investigation. Several research groups have recently reported the photoresponse and memory functions of organic thin film transistors (OTFTs) [1–9]. One such early device took advantage of the illumination of poly(3-hexylthiophene) (P3HT) with light at a wavelength of 632.8 nm to create electric charges that were later trapped at the polymer–dielectric interface [1]; this system featured an ON/OFF ratio of ca. 30 for the memory window at a gate voltage (V_{GS}) of 60 V under a light intensity of 70 mW/cm^2. This device exhibited a loss of 70% in its drain current and a short retention time after turning the light off. An alternative approach involves the use of conjugated polymers or quantum dots (QDs) as photosensitive materials along with carbon nanotube (CNT)-based field effect transistors for the fabrication of optoelectronic memory devices that function through optical programming and electrical erasing. One such memory device featuring a CNT transistor coated with poly(3-octylthiophene) (P3OT) exhibited an ON/OFF ratio of ca. 10^3 after lasing at a wavelength of 457 nm at a value of V_{GS} of 4 V under a laser power of ca. 190 mW/cm^2. For this system, a several percentage loss of the ON state current occurred 40 s after the laser light was turn off [2]. The same research group reported that for a similar device structure that exposed to a much higher laser power [3], it showed an absence of current decay after light turn-off or there exist two regimes: one decaying and one non-volatile [4]. Another optoelectronic

* Corresponding author. Tel.: +886 35 731871; fax: +886 35 724727.
E-mail address: khwei@mail.nctu.edu.tw (K.-H. Wei).

1566-1199/$ - see front matter © 2009 Elsevier B.V. All rights reserved.
doi:10.1016/j.orgel.2009.03.011

memory device, comprising a conjugated polymer coating a CNT transistor irradiated with UV light at 365 nm, provided an ON/OFF ratio of ca. 4 at a value of V_{GS} of 4 V, but with a retention time of over 16 h [5].

It appears that commercially viable TFT memory devices exhibiting high ON/OFF current ratios and long retention times (particularly when the gate voltage is turned off) are difficult to prepare. Approaches toward improving device performances while simplifying their fabrication processes are, therefore, necessary for the development and application of future commercial memory devices.

Bulk heterojunctions [10], in which n-type (e.g., fullerene) and p-type (e.g., conjugated polymer) materials are intimately mixed on the nanometer scale to form interpenetrated networks, have been adopted recently to achieve efficient photoinduced charge generation and separation [11,12]. On the other hand, semiconductor nanocrystal quantum dots (QDs) have also been used in such organic optoelectronic devices as solar cells [13] and light-emitting diodes (LEDs) [14]. Recently, the first bulk heterojunction photoresponsive OTFT memory device incorporating P3HT and CdSe QDs by our group was reported to have an ON/OFF ratio of ca. 10^2; because the CdSe QDs served as trap centers, the memory effect of the device was maintained for 1 h-even without a gating voltage [15].

Type-I core/shell structured QDs, in which the conduction and valence bands of the shell material are higher and lower, respectively, than the corresponding values of the core material, feature a quantum well structure that can confine both holes and electrons in the core [16]. Hence, the quantum well structure of such QDs enhances their electroluminescence (EL) in LED applications [17].

In this paper, we report bulk heterojunction polymer TFT memory devices exhibiting long retention times and high ON/OFF ratios that we fabricated using quantum well-structured QDs comprising CdSe cores and ZnSe shells (CdSe@ZnSe). To the best of our knowledge, this system is the first to employ a quantum well structure to enhance the memory effect of polymer TFTs.

2. Experiment

2.1. Materials

Regioregular poly(3-hexylthiophene) was obtained from Rieke Metals and used as received. Cadmium acetate dihydrate [$Cd(OAc)_2 \cdot 2H_2O$] was obtained from Fisher Chemicals. Selenium (Se, 99.999%) and hexadecylamine (HDA, tech. 90%) were obtained from Aldrich. Trioctylphosphine oxide (TOPO, 98%), *n*-octylphosphonic acid (OPA, 98%), and trioctylphosphine (TOP, tech. 90%) were purchased from Alfa Aesar. Zinc stearate was obtained from J.T. Baker. The solvents heptane, toluene, methyl alcohol, and chloroform (HPLC-grade) were obtained from commercial sources.

TOPO-capped CdSe and CdSe@ZnSe QDs were synthesized using a modification of a procedure reported previously [18,19]: A mixture of $Cd(OAc)_2 \cdot 2H_2O$ (105 mg), HDA (1.39 g), OPA (225 mg), and TOPO (1.95 g) was heated in a 25-ml three-neck flask at 270 °C under an argon flow to obtain a colorless, clear solution. At this temperature, the Se solution (100 mg in 2.4 ml TOP) was injected rapidly. The growth temperature was maintained at 270 °C for 100 s and then the reaction mixture was cooled to room temperature. The CdSe QDs were collected as powders after their precipitation with MeOH. A colloidal solution of the CdSe QDs (ca. 20 mg) in heptane (4 ml) was heated in a 25-ml three-neck flask under an argon flow. After addition of TOPO (2.5 mg) and HDA (1.5 mg), the mixture was heated at ca. 190 °C to completely remove the heptane. Zinc stearate (316 mg) was dissolved in toluene (2.5 ml) at ca. 60 °C. After cooling to room temperature, the resulting 0.2 M solution was mixed with TOP (2.5 ml) and Se (39.48 mg). This mixture was injected via syringe pump (0.085 ml/min) into the reaction flask containing the CdSe QDs at ca. 190 °C. After the addition was complete, the crystals were annealed at 190 °C for an additional 1 h. The CdSe@ZnSe QDs were collected as powders after their precipitation with MeOH.

2.2. Device fabrication and measurement

A solution of P3HT in $CHCl_3$ was blended with a solution of the QDs in $CHCl_3$; the P3HT/QD composite weight ratio was 1:0.1. The P3HT and P3HT/QD TFT devices were fabricated in a bottom-gate configuration. An n+ silicon wafer (<0.005 Ω cm) was used as the substrate and gate; 900-Å thermal SiO_2 (capacitance: 38.4 nF/cm^2) was the gate insulator; a photolithographically patterned Au/Cr layer (thickness: 600/50 Å) functioned as the source and drain electrodes (W = 1000 μm; L = 10 μm). Octadecyltrichlorosilane (OTS) was deposited by immersing the substrate in 1 mM heptane solution for 10 min; the substrates were rinsed with heptane and isopropanol, followed by drying with N_2. The P3HT and P3HT/QD films (thickness: ca. 60 nm) were deposited through spin-coating and then they were annealed at 150 °C for 5 min inside a glove box under N_2 atmosphere. The samples were then transferred to a cryogenic probe station (VFTTP4, Lakeshore). The performance of each device was measured under vacuum (<1×10^{-5} torr) in the dark using a Hewlett–Packard 4156C semiconductor parameter analyzer. The devices were illuminated under vacuum using a tungsten halogen lamp (2.75 mW/cm^2).

2.3. Characterization

TEM images were obtained using an FEI Tecnai Spirit TWIN apparatus operated at 120 keV. For TEM analysis, the devices were placed into 1% HF solution; after the active layers had floated to the solution surface, they were transferred to the TEM grid. A Hitachi U-4100 spectrophotometer was used to obtain optical absorption spectroscopy in the UV–vis range; a Hitachi F-4500 FL spectrophotometer was employed to obtain photoluminescence spectra.

3. Results and discussion

To discern the effect that the ligands on the QDs had on the performance of the memory devices, we investigated

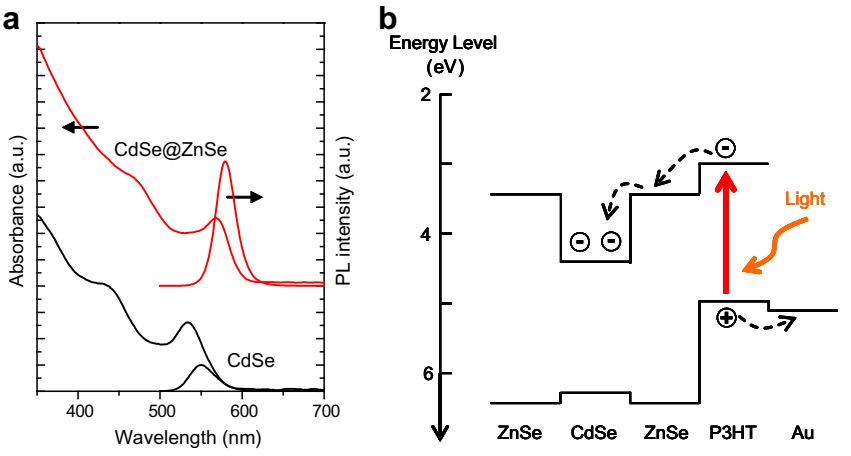

Fig. 1. (a) Absorption and photoluminescence spectra of the CdSe and CdSe@ZnSe QDs. (b) Energy level diagram for the CdSe and ZnSe bulk materials, P3HT, and the electrode materials.

trioctylphosphine oxide (TOPO) as the ligand because TOPO-capped CdSe QDs feature large barriers that prevent electron tunneling into P3HT and better dispersion than pyridine-capped CdSe QDs in P3HT (see Fig. S1, Supplementary material).

Fig. 1a presents the UV–vis and photoluminescence (PL) spectra of CdSe and CdSe@ZnSe QDs that we prepared from the same concentrations in toluene. The first excitonic absorption peak of the CdSe QDs appeared at ca. 540 nm, suggesting an average particle size of ca. 2.85 nm [20], which is consistent with the dimensions obtained from transmission electron microscopy (TEM) image analyses. The presence of the ZnSe shell caused a red shift in the absorption spectrum and enhanced the PL intensity.

Fig. 1b displays a schematic energy level diagram of the CdSe and ZnSe bulk materials, P3HT, and Au electrodes [21,22]. Because the lowest unoccupied molecular orbital (LUMO) and the highest occupied molecular orbital (HOMO) of P3HT lie above the conduction band (CB) and valance band (VB) edges of the CdSe and ZnSe materials, respectively, the P3HT–ZnSe interface forms an offset band heterojunction; in contrast, the CdSe core and ZnSe shell form a type-I heterojunction. When illuminated, excitons were generated in the QDs and P3HT, charge separation occurred at the P3HT–QDs interface, and then electrons and holes were transferred into the QDs and P3HT, respectively [23]. The work function of Au (5.1 eV) matched the HOMO of P3HT (4.9 eV); therefore, an Ohmic contact formed for hole injection, resulting in hole-only transport in the P3HT/QD TFTs.

Fig. 2a displays the transfer curves (drain-to-source voltage, $V_{DS} = -20$ V) of the P3HT-only and P3HT/QD (including CdSe and CdSe@ZnSe) bulk heterojunction TFTs in the dark and under white light (2.75 mW/cm^2). All of the devices exhibited the characteristic behavior of p-channel field-effect transistors. The hole mobility μ_h was obtained using the following equation [24]:

$$I_{DS} = \frac{W}{2L}\mu_h C(V_{GS} - V_{th})^2 \quad (1)$$

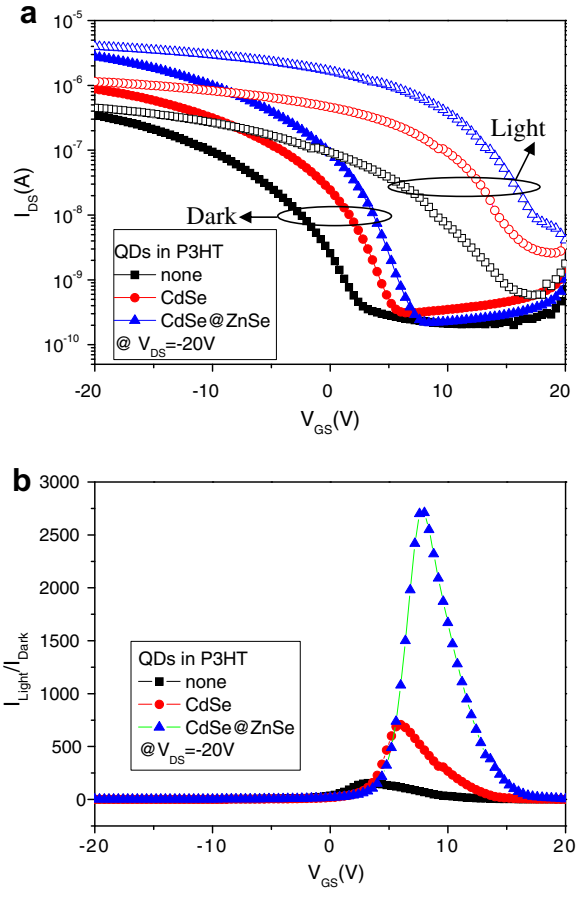

Fig. 2. (a) Transfer characteristics ($V_{DS} = -20$ V) of TFTs incorporating P3HT-only, P3HT/CdSe, and P3HT/CdSe@ZnSe blend films and operated in the dark and under white light (2.75 mW/cm^2). (b) Relative I_{light}/I_{dark} ratios of the transfer characteristics of the drain current in the dark and under white light.

where V_{th} is the threshold voltage, W is the channel width, L is the channel length, C is the gate oxide capacitance per

unit area, and V_{GS} is the gate voltage. In the saturation regime, the hole mobilities of the P3HT-only, P3HT/CdSe QD, and P3HT/CdSe@ZnSe QD devices were 4×10^{-4}, 8×10^{-4}, and 3×10^{-3} $cm^2 V^{-1} s^{-1}$, respectively. Since the HOMO of the P3HT is much higher than the VB of CdSe QDs, this energy difference constitutes a larger energy barrier that prevents holes transferring from P3HT to CdSe QDs [25]. Thus, incorporation of the CdSe and CdSe@ZnSe QDs into the P3HT enhanced the hole mobility of the devices slightly, owing to the fact that it is possible that the QDs reduced the density of traps in the polymer [the concentration of the QDs in the P3HT film was 10% (w/w)]. The hole mobility of each of these three composites was lower than that reported recently for pure P3HT (ca. 10^{-2} to 10^{-3} $cm^2 V^{-1} s^{-1}$) [26]. Note, however, that several factors, such as the molecular weight of the P3HT, its methods of preparation and purification, the channel dimensions, and the substrate treatment conditions, can influence the characteristics of a TFT device. The values of V_{th} of the P3HT-only, P3HT/CdSe QD, and P3HT/CdSe@ZnSe QD devices were 0.8, 3.4, and 3.8 V, respectively; i.e., those of the blended devices shifted to more-positive values, indicating the existence of a permanent electric field at the interface. The increase in the drain current of the polymer/QD blends under illumination resulted from accumulation of the majority carriers (holes) inside the active layer; these holes tended to drift toward the drain electrode, whereas the electrons will stay in the QDs or the insulator layer. It is well-known that the properties of the interface between the insulator and the semiconductor can critically influence the device performance. When the OTFT is illuminated, the electrons are attracted to the interface with the gate dielectric by a positive gate voltage; they are then trapped either in the dielectric layer or at the interface. Acceptor-like traps, when the traps are filled by electrons, leads to a positive threshold voltage. After turning the light off, electron detrapping under a negative gate bias indicates a returning to the initial state.

Fig. 2b present plots of the ratio I_{light}/I_{dark} versus V_{GS}. We obtained the ratio I_{light}/I_{dark} from the transfer curves of the drain current for samples either in the dark or irradiated under white light (2.75 mW/cm^2). The I_{light}/I_{dark} ratio depends on the gate bias for a given drain bias; it decreases as the gate bias is applied above or below the switch-on voltage. In the depletion regime, the maximum I_{light}/I_{dark} ratios for the P3HT-only, P3HT/CdSe, and P3HT/CdSe@ZnSe devices were 1.6×10^2, 7.1×10^2, and 2.7×10^3, respectively; i.e., the photosensitivity of the P3HT/CdSe@ZnSe device was higher than that of the P3HT-only and P3HT/CdSe devices. Because the switch-on voltages, which were defined by the maximum I_{light}/I_{dark} ratios, for the P3HT/CdSe and P3HT/CdSe@ZnSe devices were 5.6 and 8 V, respectively (Fig. 2b), we chose to operate these two devices at a value of V_{GS} of 5 V for our subsequent time-response studies.

Fig. 3a displays the evolution of the normalized drain current for the P3HT/CdSe and P3HT/CdSe@ZnSe devices at values of V_{DS} and V_{GS} of −20 and 5 V, respectively, after they were subject to a light of 2.75 mW/cm^2 with a duration of 100 s. At the onset of illumination, the drain currents of both the P3HT/CdSe and P3HT/CdSe@ZnSe devices increased dramatically, and then dropped off to form plateaus when light is turned off. After the light had been turned off for 400 s, the drain current of the P3HT/CdSe@ZnSe device had decreased by 14%, compared with a corresponding loss of 60% for the P3HT/CdSe device. We suspect that the mechanism underlying this behaviors

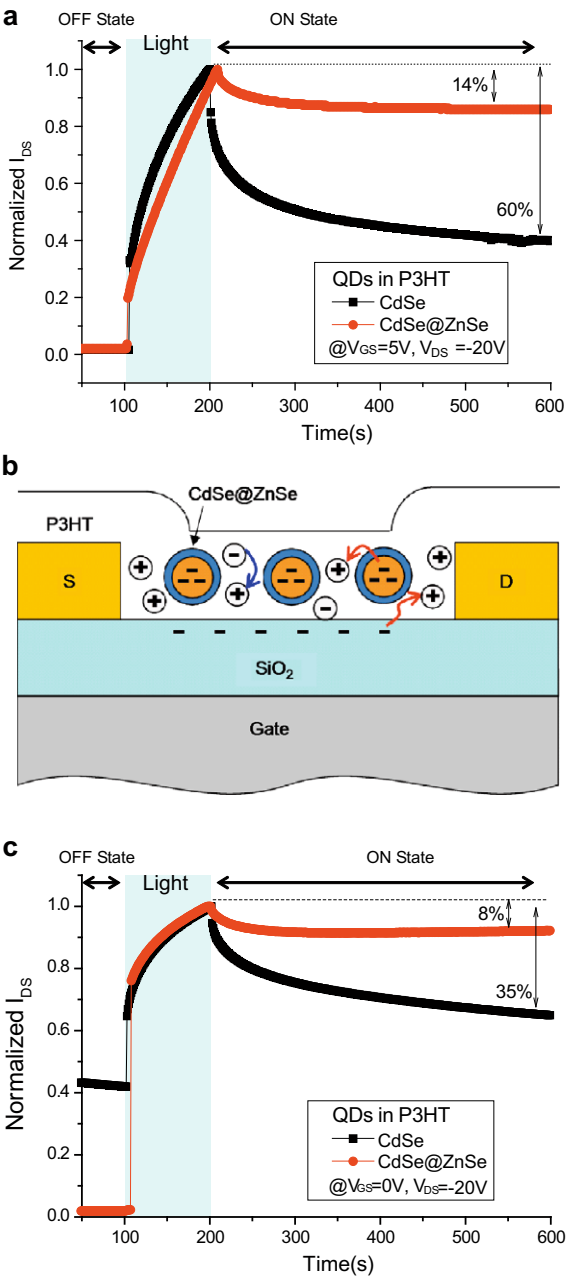

Fig. 3. Time responses of the normalized drain currents of the P3HT/CdSe and P3HT/CdSe@ZnSe devices (V_{DS} = −20 V) illuminated by a light of 2.75 mW/cm^2 with a duration of 100 s at values of V_{GS} of (a) 5 and (c) 0 V. (b) Schematic representation of the relaxation processes within the bulk heterojunction P3HT/CdSe@ZnSe active layers in TFT devices. Red: slow decay process; blue: fast decay process. (For interpretation of the references to colour in this figure legend, the reader is referred to the web version of this article.)

involved two relaxation processes: (i) rapid decay corresponding to the recombination of closely spaced charge carriers and (ii) slow decay resulting from the recombination of well-separated carriers [27] (Fig. 3b). The slow decay might be manifested by the fact that, in a heterojunction device, the spatially separated holes and electrons will move differently-the holes drifting toward the channel and then reaching the drain electrode, the electrons mostly confined in the QDs and at the P3HT-SiO_2 interface. After the light was turned off, the devices existed in a non-equilibrium state; some of the photogenerated holes presumably recombined with some residual electrons that were not confined in QDs, causing a reduction in the drain current, eventually reaching a metastable state. Because the coverage of the CdSe QDs surfaces by TOPO was only ca. 55% [21], the ZnSe shell layer between the CdSe core and the P3HT polymer in the P3HT/CdSe@ZnSe devices resulted in an additional tunneling barrier that prevented the electrons from tunneling back to P3HT, leading to a smaller decrease in the drain current and a larger retention time relative to those of the CdSe QDs devices, as indicated by the slope of the drain currents at 600 s.

Because low power consumption is an important feature for non-volatile memory applications, it is preferable to operate optoelectronic memory devices in the absence of a gate voltage. Fig. 3c displays the evolution of the normalized drain currents at values of V_{DS} and V_{GS} of −20 and 0 V, respectively, for the devices subjected to a light of 2.75 mW/cm^2 with a duration of 100 s. After turning off the light, the P3HT/CdSe@ZnSe and P3HT/CdSe devices exhibited losses of 8 and 35%, respectively, of their ON state currents, with ON/OFF ratios of 36 and 1.5, respectively. Therefore, we conclude that Type-I heterojunction core/shell QDs are more suitable than homogenous QDs for memory applications both with and without applied gate voltages.

Fig. 4 presents TEM images of the CdSe and CdSe@ZnSe QDs dispersed in the P3HT matrix at a P3HT-to-QD weight ratio of 1:0.1. The bright appearance of the P3HT regions relative to dark QD regions in the contrast image was probably due to the large difference in their respective electron densities. The CdSe QDs were distributed rather homogenously in the P3HT matrix; we suspect that the lower homogeneity of the P3HT/CdSe@ZnSe film was due to a loss of TOPO coverage during the growth of the shell. The TEM images in the insets to Fig. 4 reveal that the CdSe and CdSe@ZnSe QDs had average sizes of ca. 2.9 and 4.3 nm, respectively. The ZnSe shell thickness was ca. 0.7 nm, i.e., slightly larger than the critical penetration length of electrons (ca. 0.5 nm) [21].

To determine the optimal operating conditions, we fabricated 10 devices from three independently prepared P3HT/CdSe@ZnSe films; the optimal ON/OFF ratio was greater than 1000 at a value of V_{GS} of 10 V. Fig. 5 reveals that the P3HT/CdSe@ZnSe devices exhibited a high ON/OFF ratio of 2700 at a value of V_{GS} of 10 V-without any noticeable decay after the light had been turned off for 8000 s. This result indicates that incorporating core/shell QDs into a conjugated polymer significantly extends the lifetime of the memory states of the resulting polymer TFTs. Moreover, the inset to Fig. 5 also displays the

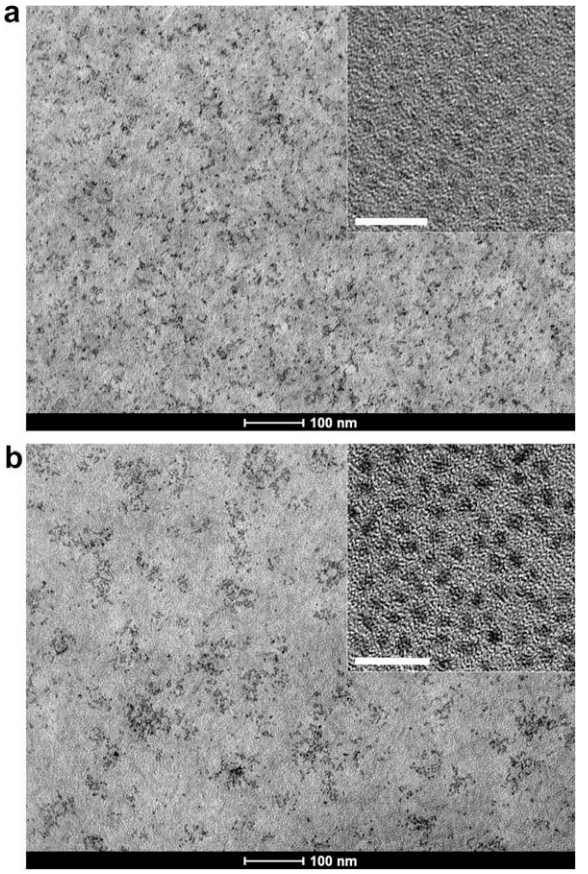

Fig. 4. TEM images of (a) the CdSe QDs and (b) the CdSe@ZnSe QDs dispersed in the P3HT matrix Insets: TEM images of the CdSe and CdSe@ZnSe QDs (scale bar: 20 nm).

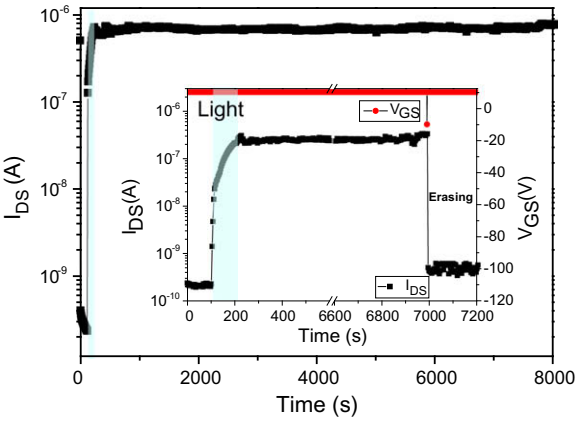

Fig. 5. Time response of the value of I_{DS} of the P3HT/CdSe@ZnSe device at V_{GS} = 10 V and V_{DS} = −20 V illuminated by a light of 2.75 mW/cm^2 with a duration of 100 s. Inset: Time response of the P3HT/CdSe@ZnSe device after a negative gate voltage pulse (V_{GS} = −10 V) was applied at 7000 s to erase the memory.

dynamic responses of the optical programming and electrical erasing of the P3HT/CdSe@ZnSe device. The ON state current could be erased effectively when using a single

pulse of the gate voltage (−10 V) for a short duration (1 s). When this negative pulse gate bias was applied, the Fermi level of CdSe and ZnSe modulated up towards the conduction band, thereby reducing the barrier height. As a result of the decrease in the barrier hight, electron jump back into the P3HT and recombine with hole. Thus, we suspect that the trapped electrons were induced by the electric field to move out of the QDs and recombine with the holes to reform the OFF state. Based on this protocol of operation, it was possible for us to program the P3HT/CdSe@ZnSe device optically and then erase it electrically.

4. Summary

In summary, we have examined the optoelectronic properties and memory effects of polymer TFTs incorporating P3HT/CdSe and P3HT/CdSe@ZnSe QDs as an active layer. After illumination, the presence of the quantum well-structured core/shell CdSe@ZnSe quantum dots in the P3HT film substantially enhanced the ON/OFF ratio to 2700, maintaining this value for 8000 s without noticeable decay. This fabrication approach opens up the possibility of improving the memory performance of polymeric materials prepared at low cost using simple processes.

Acknowledgements

We thank the National Science Council of Taiwan for funding (NSC 97-2120-M-009-006) and (NSC97-2218-E009-004).

Appendix A. Supplementary material

Supplementary data associated with this article can be found, in the online version, at doi:10.1016/j.orgel.2009.03.011.

References

[1] S. Dutta, K.S. Narayan, Adv. Mater. 16 (2004) 2151.
[2] J. Borghetti, V. Derycke, S. Lenfant, P. Chenevier, A. Filoramo, M. Goffman, D. Vuillaume, J.P. Bourgoin, Adv. Mater. 18 (2006) 2536.
[3] J.P. Bourgoin, J. Borghetti, P. Chenevier, V. Derycke, A. Filoramo, L. Goux, M.F. Goffman, S. Lyonnais, K. Nguyen, G. Robert, S. Streiff, J.M. Bethoux, H. Happy, G. Dambrine, S. Lenfant, D. Vuillaume, Proc. Int. Electron. Dev. Meeting (2006) 435.
[4] C. Anghel, V. Derycke, A. Filoramo, S. Lenfant, B. Giffard, D. Vuillaume, J.-P. Bourgoin, Nano Lett. 8 (2008) 3619.
[5] A. Star, Y. Lu, K. Bradley, G. Grüner, Nano Lett. 4 (2004) 1587.
[6] L. Hu, Y.L. Zhao, K. Ryu, C. Zhou, J.F. Stoddart, G. Grüner, Adv. Mater. 20 (2008) 939.
[7] S. Dutta, K.S. Narayan, Phys. Rev. B: Condens. Matter Mater. Phys. 68 (2003) 125208.
[8] K.S. Narayan, M. Rao, R. Zhang, P. Maniar, Appl. Phys. Lett. 88 (2006) 243507.
[9] Y. Shi, H. Tantang, C.W. Lee, C.H. Weng, X. Dong, L.J. Li, P. Chen, Appl. Phys. Lett. 92 (2008) 103310.
[10] (a) N.S. Sariciftci, L. Smilowitz, A.J. Heeger, F. Wudl, Science 258 (1992) 1474;
(b) G. Yu, J. Gao, J.C. Hummelen, F. Wudl, A.J. Heeger, Science 270 (1995) 1789.
[11] N. Marjanovic, T.B. Singh, G. Dennler, S. Gunes, H. Neugebauer, N.S. Sariciftci, R. Schwodiauer, S. Bauer, Org. Electron. 7 (2006) 188.
[12] S.M. Mok, F. Yan, H.L.W. Chan, Appl. Phys. Lett. 93 (2008) 023310.
[13] W.U. Huynh, J.J. Dittmer, A.P. Alivisatos, Science 295 (2002) 2425.
[14] M. Gao, B. Richter, S. Kirstein, Adv. Mater. 9 (1997) 802.
[15] C.C. Chen, M.Y. Chiu, J.T. Sheu, K.H. Wei, Appl. Phys. Lett. 92 (2008) 143105.
[16] X. Peng, M.C. Schlamp, A.V. Kadavanich, A.P. Alivisatos, J. Am. Chem. Soc. 119 (1997) 7019.
[17] (a) J. Lim, S. Jun, E. Jang, H. Baik, H. Kim, J. Cho, Adv. Mater. 19 (2007) 1927;
(b) Z. Tan, F. Zhu, J. Xu, A.Y. Wang, J.D. Dixon, L. Li, Q. Zhang, S.E. Moheney, J. Ruzyllo, Nano Lett. 7 (2007) 3803;
(c) M.T. Harrison, S.V. Kershaw, A.L. Rogach, A. Kornowski, A. Eychmuller, H. Weller, Adv. Mater. 12 (2000) 123.
[18] H. Skaff, K. Sill, T. Emrick, J. Am. Chem. Soc. 126 (2004) 11322.
[19] P. Reiss, J. Bleuse, A. Pron, Nano Lett. 2 (2002) 781.
[20] W.W. Yu, L. Qu, W. Guo, X. Peng, Chem. Mater. 15 (2003) 2854.
[21] J. Bleuse, S. Carayon, P. Reiss, Physica E 21 (2004) 331.
[22] S. Cho, J. Yuen, J.Y. Kim, K. Lee, A.J. Heeger, Appl. Phys. Lett. 90 (2007) 063511.
[23] N.C. Greenham, X. Peng, A.P. Alivisatos, Phys. Rev. B 54 (1996) 17628.
[24] G. Horowitz, Adv. Mater. 10 (1998) 365.
[25] Z.X. Xu, V.A.L. Roy, P. Stallinga, M. Muccini, S. Toffanin, H.F. Xiang, C.M. Che, Appl. Phys. Lett. 90 (2007) 223509.
[26] R.J. Kline, M.D. McGehee, E.N. Kadnikova, J. Liu, M.J. Frechet, Adv. Mater. 15 (2003) 1519.
[27] K.S. Narayan, N. Kumar, Appl. Phys. Lett. 79 (2001) 1891.